Soft Comput (2005) 9: 793–802
DOI 10.1007/s00500-004-0420-5

FOCUS

T. M. Blackwell

Particle swarms and population diversity

Published online: 13 May 2005

Abstract The optimisation of dynamic optima can be a difficult problem for evolutionary algorithms due to diversity loss. However, another population based search technique, particle swarm optimisation, is well suited to this problem. If some or all of the particles are 'charged', an extended swarm can be maintained, and dynamic optimisation is possible with a simple algorithm. Charged particle swarms are based on an electrostatic analogy—inter-particle repulsions enable charged particles to swarm around a nucleus of neutral particles. This paper proposes a diversity measure and examines its time development for charged and neutral swarms. These results facilitate predictions for optima tracking given knowledge of the amount of dynamism. A number of experiments test these predictions and demonstrate the efficacy of charged particle swarms in a simple dynamic environment.

1 Introduction

Particle swarm optimisation (PSO) is a population based optimisation technique inspired by models of swarm and flock behaviour (Kennedy and Eberhart 1995). Although PSO has much in common with evolutionary algorithms, it differs from other approaches by the inclusion of a solution (or particle) velocity. New potentially good solutions are generated by adding the velocity to the particle position. Particles interact with other particles in the population (swarm) through two accelerations. These accelerations are spring-like: each particle is attracted to its previous best position, and to the global best position attained by the swarm, where 'best' is quantified by the value of an objective function at that position. These swarms have proven to be very successful in finding global optima in various static contexts such as the optimisation of certain benchmark functions (Eberhart and Shi 2001).

Evolutionary techniques have been applied to the dynamic problem (Branke 2001, 2003). The application of PSO techniques is a new area and results for environments of low spatial severity are encouraging (Eberhart and Shi 2001; Carlisle and Dozier 2000). Evolutionary and PSO algorithms, in a dynamic context, can suffer from over-specialization. In general, they require further adaptations so that they can detect change, and then respond to it. Some possible adaptations of the PSO have been studied (Hu and Eberhart 2002), but these adaptations remain arbitrary. A different extension of PSO, which solves the problem of change detection and response, has been suggested by Blackwell and Bentley (Blackwell and Bentley 2002). In charged-PSO (CPSO), some or all of the particles have, in analogy with electrostatics, a 'charge'. A third collision-avoiding acceleration is added to the particle dynamics, by incorporating electrostatic repulsion between charged particles. This repulsion maintains population diversity, enabling the swarm to automatically detect and respond to change, yet does not diminish greatly the quality of solution. In particular, it works well in certain spatially severe environments (Blackwell and Bentley 2002). Entirely charged swarms and swarms with 50% of their members charged have been compared with adapted PSO and random search in a variety of dynamic contexts, including cases of very high spatial and temporal severity (Blackwell 2003).

Much of the understanding of the behaviour of particle swarms is of an empirical nature, but a paper by Clerc and Kennedy advances theoretical knowledge by proving convergence for a simplified model (Clerc and Kennedy 2002). This simplified one-dimensional model is for non-interacting particles and hence does not optimise anything. For optimisation, particle interactions

T. M. Blackwell
Department of Computing Goldsmiths College,
University of London, New Cross,
London, SE14 6NW, UK
E-mail: t.blackwell@gold.ac.uk
Tel.: +44-20-79197859
Fax: +44-20-79197853

need to be included so that knowledge of a good position found by a particle (i.e. potentially good solutions) can be communicated to other particles.

This paper extends the work of Clerc and Kennedy to include particle interactions. It is suggested here that the maximum component separation of the particle positions in the swarm is a suitable diversity measure. For neutral (i.e. uncharged) swarms, the rate of contraction of $|S|$ can then be compared to the change in optimum position.

A limit is also suggested for $|S^+|$, the diversity of a charged swarm. The balance of electrostatic repulsion between charged particles and the attraction to the best positions will maintain the charged population diversity at a fixed level, so that hopefully optimum jumps on any time scale can be tracked, if they occur within $|S^+|$.

The CPSO algorithm is defined and the background to Clerc and Kennedy's proof is covered in the next section. Section 3 defines $|S|$ and obtains estimates for the simplified model of Clerc and Kennedy, and also for the inclusion of particle interactions and spring randomisation (PSO). Some qualitative predictions about charged swarm diversity are also made in this section and some upper and lower bounds calculated. Experiments to illustrate PSO and CPSO diversity and performance in a dynamic environment are presented in Sect. 4. The paper ends with a discussion of the theoretical and experimental results.

2 Particle swarm algorithms and convergence

2.1 CPSO algorithm

A swarm of $i = 1,...,N$ particles is a set of positions $\mathbf{x}_i$ and velocities $\mathbf{v}_i$, $S = \{\mathbf{x}_i, \mathbf{v}_i\}$ where each vector $\mathbf{x}_i$, $\mathbf{v}_i$, has $j = 1,...,d$ components. Throughout this paper, d-dimensional vectors will always be written in bold lower case (e.g. $\mathbf{a}$) with (Euclidean) norm $|\mathbf{a}| = a$ and x_{ij}, v_{ij} refer to the j'th component of $\mathbf{x}_i$ and $\mathbf{v}_i$ respectively. Particle update consists of updating the particle velocity by adding an acceleration to the current velocity and adding this updated velocity to the current position. The acceleration is a simple spring-like attraction to an attractor $\mathbf{p}_i$ (spring constant φ_1), which may differ for each particle, and to the attractor $\mathbf{p}_g$ (spring constant φ_2) of the best performing particle (index g) in some neighbourhood (which may be the whole swarm). The particles interact by modifying attractors $\mathbf{p}_i$. This modification, which is the essence of what may be termed swarm intelligence, arises from the evaluation of an objective function f at $\mathbf{x}_i$, and is labelled attractor update in Table 1.

The outline of the CPSO algorithm is given in Table 1. Positions and velocities are initialised in a search space $[-X/2, X/2]^d$ where X is the dynamic range of the variables in each dimension. A single iteration (numerated by the variable t) consists of a complete pass through the swarm, updating positions and velocities and attractors.

In the particle update, χ is a constriction factor, chosen to ensure convergence, and $\xi_{1,2}$ are random numbers drawn uniformly from the interval [0, 1] effectively randomising the spring constants in the interval $[0, \phi_{1,2}]$ at each iteration. Table 1 also shows an additional repulsive acceleration $\mathbf{a}_i = \sum_{k \neq i} \mathbf{a}_i(k)$, where

$$\mathbf{a}_i(k) = \begin{cases} \frac{Q_i Q_k}{|\mathbf{x}_i - \mathbf{x}_k|^3}(\mathbf{x}_i - \mathbf{x}_k), & r_c \le |\mathbf{x}_i - \mathbf{x}_k| \le r_p \quad \text{(1a)} \\ \frac{Q_i Q_k}{r_c^2}\frac{(\mathbf{x}_i - \mathbf{x}_k)}{|\mathbf{x}_i - \mathbf{x}_k|}, & |\mathbf{x}_i - \mathbf{x}_k| < r_c \quad \text{(1b)} \\ 0, & |\mathbf{x}_i - \mathbf{x}_k| > r_p \quad \text{(1c)} \end{cases} \tag{1}$$

and i, k are particle indices. The PSO algorithm is therefore a special case of CPSO, where every particle is uncharged, $Q_i = 0$ (neutral CPSO).

Avoidance is only between pairs of particles that have non zero charge Q, and is Coulomb-like in the shell $r_c \le r \le r_p$ (Eq. 1a). At separations less than the core radius r_c, the repulsion is fixed at the value at the core radius (Eq. 1b), and there is no avoidance for separations beyond the perception limit of each particle, r_p(Eq. 1c). The core radius serves to tame the repulsion at small separations and prevent large accelerations which would place charged particle outside the search space. Notice that the particle repulsion $\mathbf{a}_i$ is determined before the update of each component $\mathbf{x}_i$. This is because the Coulomb law, unlike the spring laws used for the attractive accelerations, depends on the Euclidean separation $|\mathbf{x}_i - \mathbf{x}_k|$ and not on the component separation $|x_{ij} - x_{kj}|$, and so cannot be implemented inside the loop indexed by j in Table 1.

2.2 Convergence proof for the simplified model

The convergence proof of Clerc and Kennedy is for a simplified one-dimensional model without interaction and with fixed springs (Clerc and Kennedy 2002).

Table 1 Particle swarm algorithm for charged and neutral swarms

```
CPSO
initialise S(0) = {x_i, v_i} in cube [-X/2, X/2]^d
g=1, t=1
for i=1 to population size N
 p_i = x_i
 if f(p_i) < f(p_g) then g = i
next i
do
 for i = 1 to population size N
  calculate a_i(t)
  // particle update
  for j=1 to dimension size d
   v_ij(t+1)=χ{v_ij(t)+ξ1φ1[p_ij(t)−x_ij(t)]+ξ2φ2[p_gj(t)−x_ij(t)]}+a_ij(t)
   x_ij(t+1)=x_ij(t)+v_ij(t+1)
  next j
  // attractor update
  if f(x_i(t+1)) <f(p_i(t+1)) then p_i(t+1) = x_i(t+1)
     else p_i(t+1)=p_i(t)
   if f(p_i(t+1)) < f(p_g) then g = i
 t++
 next i
until termination criterion is met
```

The algorithm is set out in Table 2.

Since there are no interactions in this model, the dynamics can be analysed by considering a one-dimensional dynamic system with fixed attractor p and fixed spring constant φ

$$v(t+1) = v(t) + \phi[p - x(t)]$$
$$x(t+1) = x(t) + v(t) + \phi[p - x(t)] \tag{2}$$

Velocity constriction, which takes the place of velocity clamping in older versions of PSO, is applied by scaling $v(t+1)$ by a factor $\chi < 1$:

$$v(t+1) = \chi\{v(t) + \phi[p - x(t)]\}$$
$$x(t+1) = x(t) + \chi\{v(t) + \phi[p - x(t)]\} \tag{3}$$

For simplicity, this is rewritten by Clerc and Kennedy as

$$v(t+1) = \chi\{v(t) + \phi y(t)\}$$
$$y(t+1) = y(t) + \chi\{-v(t) - \phi y(t)\} \tag{4}$$

or in matrix form as

$$\mathbf{P}(t+1) = \mathbf{MP}(t) \tag{5}$$

where $y(t) = p - x(t)$, $\mathbf{P}(t) = [\, v(t), y(t)]^{\mathrm{T}}$ and $\mathbf{M}$ is the 2×2 transformation matrix defined by the matrix equation

$$\begin{bmatrix} v(t+1) \\ y(t+1) \end{bmatrix} = \begin{bmatrix} \chi & \chi\phi \\ -\chi & 1 - \chi\phi \end{bmatrix} \begin{bmatrix} v(t) \\ y(t) \end{bmatrix}. \tag{6}$$

$\mathbf{M}$ is diagonalized by the similarity transform $\mathbf{A}$,

$$\mathbf{AMA}^{-1} = \mathbf{L} = \begin{bmatrix} e_1 & 0 \\ 0 & e_2 \end{bmatrix}. \tag{7}$$

The convergence conditions for χ and ϕ are obtained by noting that $||\mathbf{P}(t)||$ increases as $||\mathbf{M}^t\mathbf{P}(0)|| = ||\mathbf{L}^t \mathbf{AP}(0)||$ where $||\cdot||$ is, for example, the Euclidean norm. Clerc and Kennedy show that the eigenvalues $e_{1,2}$ are complex and of modulus $\sqrt{\chi}$ for $\varphi > 4$, with χ given by

$$\chi = \frac{2}{\phi - 2 + \sqrt{\phi^2 - 4\phi}}. \tag{8}$$

Convergence will follow if the constriction factor for a given spring constant ϕ is given by Eq. 8.

3 Diversity measure for particle swarms

3.1 Simplified model

The above result can be used to estimate the maximum component separation of the swarm S of N non-interacting particles (labelled $i = 1,\ldots,N$) moving in $j = 1,\ldots,d$ dimensions. The *diversity* of S at iteration t will be written $|S|$ (not a norm) and is defined as the maximum distance between position components j:

$$|S| = \max_j(\max_i\{x_{ij}\} - \min_i\{x_{ij}\}). \tag{9}$$

Introducing now a set of fixed attractors $\{\mathbf{p}_i\}$, one for each particle, then each component x_{ij} is subject to the simplified model and convergence entails that $y_{ij} = p_{ij} - x_{ij} \rightarrow 0$.

In this paper, a point at $\mathbf{y}$ is considered to be *inside* a set of points $\{\mathbf{x}_i\}$ if each component y_j satisfies

$$\min_i\{x_{ij}\} \leq y_j \leq \max_i\{x_{ij}\}, \tag{10}$$

and the set $\{\mathbf{y}_i\}$ is inside $\{\mathbf{x}_i\}$ if (Eq. 10) is true for each $\mathbf{y}_i$.

The distance of particle i, position component j, from attractor $\mathbf{p}_i$ provides an estimate of $|S|$:

$$|S| \sim \max_{ij}(2|y_{ij}|). \tag{11}$$

If $\{\mathbf{p}_i\}$ are within the swarm, and the attractors are tightly bunched then (Eq. 11) will be a good estimate of $|S|$. A typical configuration with tightly bunched attractors (triangles) is illustrated in Fig. 1. If, though, $\{\mathbf{p}_i\}$ are outside the swarm, $\max_{ij}(2|y_{ij}|)$ will over-estimate $|S|$. This would be the case for unusual configurations where the swarm is undergoing collective oscillations about $\{\mathbf{p}_i\}$ (Fig. 2). (Configurations can also be imagined where (Eq. 11) underestimates $|S|$, for example if each particle is close to its attractor, but the swarm is very diffuse.)

In the non-interacting simplified model, each $|y_{ij}|$ is converging to 0 as $\left(\sqrt{\chi}\right)^t$, which leads to a prediction for $|S|$ as a function of time t (measured in iterations):

$$|S| = \text{const} \times \left(\sqrt{\chi}\right)^t. \tag{12}$$

This can also be written as a *scaling law*:

$$|S(t+1)| = \text{const} \times \sqrt{\chi}|S(t)|. \tag{13}$$

3.2 Interacting particles

In PSO, interactions amongst the particles lead to attractor updates and the analysis of Sect. 3.1 does not apply. The particle update rules given in Eq. 3 become, for interacting particles (see Table 1 for neutral particles),

Table 2 The simplified model one-dimensional non-interacting model

```
Simplified model
initialise S = {x_i, v_i} in cube [-X/2, X/2]^d
do
 for i = 1 to population size (N)
  for j = 1 to dimension size (d)
   v_ij = χ(v_ij + φ(p_j − x_ij))
   x_ij = x_ij + v_ij
  next j
 next i
until termination criterion is met
```

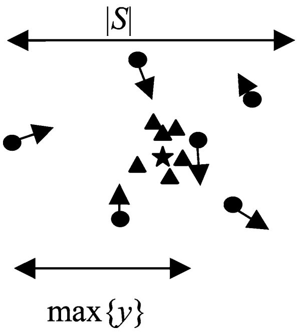

Fig. 1 Attractors lying within swarm. An optimum (*star*) lies within the attracting group

$$\mathbf{v}_i(t+1)=\chi\{\mathbf{v}_i(t)+\phi_1\xi_1[\mathbf{p}_i-\mathbf{x}_i(t)]+\phi_2\xi_2[\mathbf{p}_g-\mathbf{x}_i(t)]\}$$
$$\mathbf{x}_i(t+1)=\mathbf{x}_i(t)+\chi\{\mathbf{v}_i(t)+\phi_1\xi_1[\mathbf{p}_i-\mathbf{x}_i(t)]+\phi_2\xi_2[\mathbf{p}_g-\mathbf{x}_i(t)]\} \tag{14}$$

In fact each particle component $\mathbf{x}_{ij}$ satisfies the simplified form of Eq. 2; define

$$\begin{aligned}\tilde{\mathbf{p}}_i &= \tfrac{\xi_1\phi_1\mathbf{p}_i+\phi_2\xi_2\mathbf{p}_g}{\xi_1\phi_1+\phi_2\xi_2}\\ \tilde{\phi} &= \xi_1\phi_1+\phi_2\xi_2\end{aligned} \tag{15}$$

and substitute $\tilde{p}_{ij} \to p$, $\tilde{\phi} \to \phi$. For the moment, consider the case of fixed springs, $\xi_{1,2}=1$. (PSO is invariably run with equal spring constants, $\varphi_2 = \varphi_1$ so that $\tilde{p}_{ij}$ is midway between p_{ij} and p_{gj}.) Particle interactions mean that the $\tilde{\mathbf{p}}_i'$s change due to information sharing, and the analysis which follows Eq. 2 does not hold. In order to account for information sharing, consider particle i at iteration t; $\mathbf{p}_i$ and/or $\mathbf{p}_g$ may have changed due to updates to attractors $i,...,N$ at iteration t-1 and attractors 1,...,i-1 at iteration t so that $\tilde{\mathbf{p}}_i(t)$ changes by an amount

$$\delta\tilde{\mathbf{p}}_i(t) = \frac{\phi_1}{\phi}\delta\mathbf{p}_i + \frac{\phi_2}{\phi}\delta\mathbf{p}_g, \tag{16}$$

and $|\delta\tilde{\mathbf{p}}_i(t)| < \max\{|\delta\mathbf{p}_i|, |\delta\mathbf{p}_g|\}$. This change can be implemented mathematically by holding $\{\mathbf{p}\}_i$ fixed and shifting coordinates $\mathbf{y}_i \leftarrow \mathbf{y}_i + \delta\tilde{\mathbf{p}}_i(t)$ or in matrix form by multiplying $\mathbf{P}_i(t)$ by $\Delta(t)$ where

$$\begin{aligned}\Delta_{ij}(t) &= \begin{bmatrix}1 & 0\\ 0 & 1+\delta_{ij}(t)\end{bmatrix},\\ \delta_{ij}(t) &= \tfrac{\delta\tilde{p}_{ij}(t)}{y_{ij}(t)}.\end{aligned} \tag{17}$$

Particle update is therefore represented in matrix form as $\mathbf{P}_i(t+1) = \mathbf{M}\Delta(t)\mathbf{P}_i(t)$. Hence, with the definition $\delta_t \equiv \max_{ij}\delta_{ij}(t)$,

$$||\mathbf{P}_i(t+1)|| < (1+\delta_t)||\mathbf{MP}_i(t)||. \tag{18}$$

It is hard to place bounds on δ_t for a general objective function f due to the chaotic motion of the particles and the variety of neighbourhoods around the critical points of f. For example, a particle may approach $\tilde{\mathbf{p}}_i(t)$ arbitrarily closely, and, for finite $\delta\tilde{\mathbf{p}}_i(t)$, δ_t would become arbitrarily large. In order to proceed, therefore, two assumptions will be made.

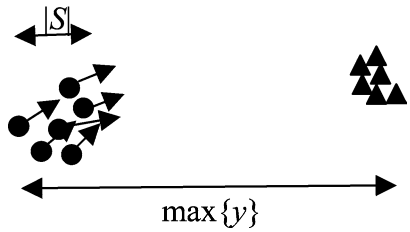

Fig. 2 Collective oscillation of particles about an attracting group lying outside the swarm

1. *Spherical symmetry*: suppose at an iteration t_0 the configuration of the swarm and attractors resembles Fig. 1. The optimum $\mathbf{x}_a$ of f is surrounded by a spherically symmetric neighbourhood D_a which the swarm does not leave for subsequent iterations, and $\mathbf{x}_a$ is the only stationary point in D_a. Spherical symmetry then implies that $\mathbf{p}_i$ will only be updated to a particle position $\mathbf{x}_i \in D_a$ if $|\mathbf{x}_i - \mathbf{x}_a| < |\mathbf{p}_i - \mathbf{x}_a|$. In other words, any updates cause the attracting group to shrink in towards $\mathbf{x}_a$, and the swarm to shrink in towards the attracting group.
2. *Scale invariance*: this is the assumption that the attracting group and the swarm shrink at the same rate so that a scaling law similar to Eq. 13 applies. In order to motivate this assumption, note that, near spherically symmetry optima, the problem is not characterised by any external length scale. This is because attractor update only depends on finding a position closer to $\mathbf{x}_a$; the details of f are unimportant within D_a. If the swarm and the attracter group are shrinking, then this would imply that the dimensionless quantity δ_t is, on average, independent of time. In other words, when averaged over initial configurations $S(t_0)$, δ_t is time (and scale) independent, $\langle\delta_t\rangle = \delta$.

To summarise, it is conjectured that convergence in locally spherically symmetric environments follows a scaling law,

$$||\mathbf{P}(t)|| < (1+\delta)||\mathbf{MP}(t-1)||, \tag{19}$$

so that $|S|$ decreases as

$$|S| \approx [(1+\delta)\sqrt{\chi}]^t = (\sqrt{\eta\chi})^t. \tag{20}$$

where $\eta = (1+\delta)^2$ is a constant positive (renormalisation) factor which multiplies the constriction χ. Convergence therefore requires that $\eta\chi < 1$.

So far, the discussion has been restricted to fixed springs. If random springs are used, Eq. 15 becomes, for $\varphi_2 = \varphi_1$,

$$\begin{aligned}\tilde{\mathbf{p}}_i &= \tfrac{\xi_1\mathbf{p}_i+\xi_2\mathbf{p}_g}{\xi_1+\xi_2}\\ \tilde{\phi} &= \phi_1(\xi_1+\xi_2)\end{aligned} \tag{21}$$

where $\xi_{1,2} \in U(0, 1)$.

Spring randomisation places $\tilde{p}_{ij}$ between p_{ij} and p_{gj} and randomises $\tilde{\phi}$ in [0, $2\varphi_1$]. The former amounts to another coordinate shift and a similar analysis leading up to Eq. 20 would ensue, except that $\langle\cdot\rangle$ would be an average over starting configurations *and* sequences of random numbers. Randomisation of $\tilde{\phi}$ is more difficult to consider in the present formalism; however Clerc and Kennedy demonstrate that $\tilde{\phi}<4$ for the simplified model leads to cyclic or quasi-cyclic particle trajectories. This could have the effect of slowing swarm contraction in the interacting case or inducing fluctuations around exponential collapse, or possibly both.

3.3 Charged particles

All charged particles mutually repel according to the modified Coulomb-like accelerations of Eq. 1. In addition, each particle is attracted towards its own $\tilde{\mathbf{p}}_i$. Suppose that the attractors are converging on the optimum $\mathbf{x}_a$. The charged sub-swarm will not collapse because as the particles get closer to $\mathbf{x}_a$, they will also get closer to each other, thus increasing the inverse square repulsions between the particles. It is expected, therefore, that the diversity of the charged swarm will settle into an 'equilibrium' value where the attractive and repulsive accelerations are, on average, in balance. However, the charged particles are involved in multiple interactions (a many-body problem) so the dynamics will be very unpredictable, chaotic even, and there could be large fluctuations about the average charged swarm size $|S^+|$ on small time scales. Here we can only make some general comments about the charged swarm diversity.

Consider two particles, one of which is stationary and close to $\mathbf{x}_a = \mathbf{O}$. The equilibrium position, R, for the second particle is the solution of $\mathbf{a}_{\text{attraction}}(\mathbf{x})+\mathbf{a}_{\text{repulsion}}(\mathbf{x})=0$, where $\mathbf{a}_{\text{attraction}} = \chi\tilde{\varphi}\mathbf{x}$ and $\mathbf{a}_{\text{repulsion}}(\mathbf{x})$ is given by Eq. 1. There are three possibilities, depending on the neutral spring constant $\chi\tilde{\phi}$, and the electrostatic constants $\gamma_c=Q^2/r_c^3$ and $\gamma_p=Q^2/r_p^3$:

1. $\gamma_c<\chi\tilde{\phi}$: there is an equilibrium position at $R = r_c\left(\frac{\gamma_c}{\chi\tilde{\phi}}\right), \quad R<r_c$
2. $\gamma_p<\chi\tilde{\phi}<\gamma_c$: there is an equilibrium position at $R = \left(\frac{Q^2}{\chi\tilde{\phi}}\right)^{1/3}, \quad r_c<R<r_p$
3. $\chi\tilde{\phi}<\gamma_p : R = r_p$ divides regions of repulsion, $x < r_p$, from attraction, $x > r_p$.

R is an estimate of the inter-particle spacing in a charged swarm of M^+ particles. It underestimates the average spacing because the above analysis does not take into account particle velocity and many body effects which would increase R. This estimate therefore suggests a lower bound to $|S^+|$:

$$|S^+|_{\text{lower}}\approx (M^+)^{1/d}R. \tag{22}$$

The amplitude of large fluctuations around the average swarm size $<|S^+|>$ can be estimated by considering the largest electrostatic acceleration that a charged particle might experience. This would occur in the (unlikely) instance that M^+-1 particles are within r_c of a particle close to the edge of the swarm, and all the acceleration vectors are parallel. The maximum acceleration is M^+-1 times the core acceleration, $a_c = \gamma_c r_c$, which gives an upper bound

$$|S^+|_{\text{upper}} \approx \langle S^+\rangle + (M^+ - 1)a_c. \tag{23}$$

4 Experiments

A series of experiments was devised to test some of the conjectures of the proceeding section. There are three groups of experiments. In group 1, four experiments (numbers 1–4) investigate the effects of particle interactions, random spring and particle charge on the diversity of neutral swarms. The second group, experiments 5 and 6, measure charged swam size for two different core radii. Finally, two experiments examine the efficacy of neutral and charged swarms in tracking a moving optimum.

Swarm composition is described as (N, M^+) where N(M^+) is the number of neutral (charged) particles. All experiments are in $d=3$ dimensions and for a dynamic range $X=10$. The spring constants in all experiments are set to the 'standard values' commonly found in the literature [Clerc and Kennedy 2002], $\varphi_{1,2}=2.05$. The constriction factor for these standard values is $\chi=0.729843788$ (Eq. 8). The parameter settings and experimental details are summarised in Tables 3 and 4. The objective function f for all experiments involving particle interactions is the sphere function $f_{\text{sph}}(\mathbf{x}) = \mathbf{x.x}$.

4.1 Diversity measure for neutral particles

4.1.1 Experiment design

The first experiment in this group sets up the conditions for Clerc–Kennedy convergence by implementing the simplified model (no interactions between the particles) with a 20 particle neutral swarm and a fixed attractor $\mathbf{p}$ at $\mathbf{O}$. Experiments 2 and 3 examine the effects of introducing particle interactions or spring randomisation and into the simplified model. The fourth experiment examines diversity change when both particle interactions and randomisation are included (standard PSO).

The swarms were released with a random configuration in $[-X/2, X/2]^3$ and the swarm size, $|S|$, was recorded at the end of each iteration t for a total of 1,000 iterations. This constitutes a single run. In total, 50 runs were conducted for each experiment, with different initial swarm configurations and, for experiments 3 and 4, different sequences of pseudo-random numbers ξ (Eq. 21).

Table 3 Description of experiments 1–8

ID	Swarm	Description
1	(20, 0)	Simplified model
2	(20, 0)	Particle interactions
3	(20, 0)	Simplified model + random springs
4	(20, 0)	Particle interactions + random springs
5	(20, 20^+)	Particle interactions, charged swarm ($r_c = 1.0$) (CPSO)
6	(20, 20^+)	Particle interactions, charged swarm ($r_c = 0.1$)(CPSO)
7	(40, 0)	Optimum tracking (PSO)
8	(20, 20^+)	Optimum tracking (CPSO) ($r_c = 1.0$)

Table 4 Fixed CPSO parameters

d	X	$\varphi_{1,2}$	χ	$\xi_{1,\,2}$	r_p	Q_i
3	10	2.05	0.729843788	$U(0, 1)$	10	1.0

4.1.2 Results and analysis

Figures 3, 4, 5, and 6 show $|S(t)|$ for a single run of experiments 1–4. The figure caption gives the equation of the best fit straight line.

These figures are typical of any of the 50 runs. Table 5 shows the gradient (standard error) and convergence factor of the best fit straight line when averaged over all runs. There is clear evidence of exponentially decaying neutral swarm size with spring randomisation inducing more fluctuations. The empirical law derived from these results is

$$|S| = k\alpha^t, \tag{24}$$

k and α constants, which agrees with the predicted form of Eqs. 12 and 20. α is related to the renormalized constriction by $\eta\chi = \alpha^2$. Table 5 shows the gradient (standard error) and convergence factor of the best fit straight line when averaged over all runs.

Experiment 1 (simplified model) is in very good agreement with the prediction of Eq. 12: $|S| = k \times \left(\sqrt{0.729843788}\right)^t = k \times 0.854308953^t$. Experiments 2–4 show that when spring randomisation, or particle interactions, or both, are included back into the simplified model, convergence is slowed down, and in fact is quite close to non-convergence, $\alpha = 0.92$–0.93. For a particular run, spring randomisation induces fluctuations around scaling which helps explain why randomisation has already proven to be beneficial for static optimisation (Kennedy and Eberhart 1995).

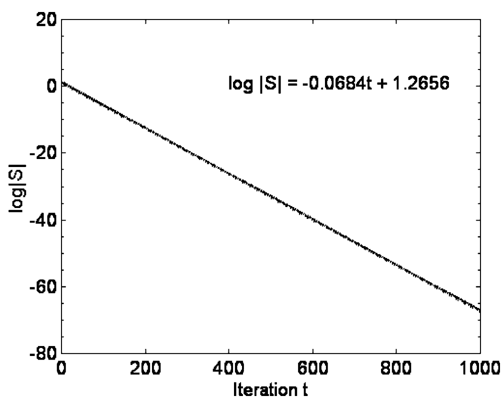

Fig. 3 Experiment 1—simplified model

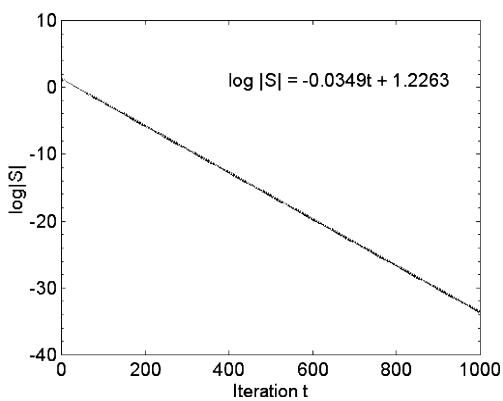

Fig. 4 Experiment 2—particle interactions

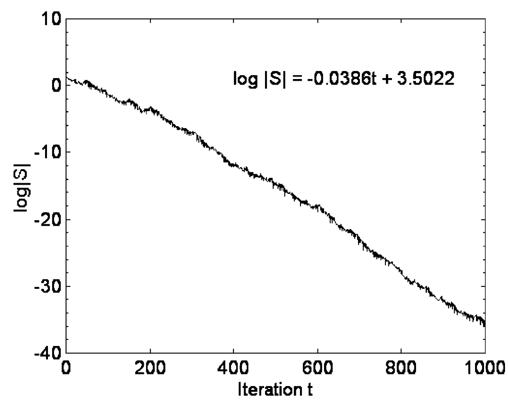

Fig. 5 Experiment 3—random springs

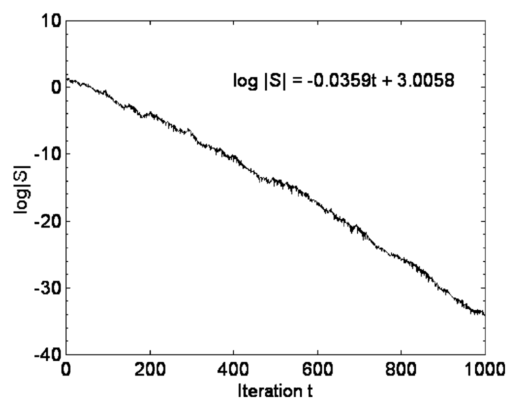

Fig. 6 Experiment 4—PSO

Table 5 Gradient (standard error) and convergence factor α for neutral swarm experiments 1–4, averaged over 50 runs

	Experiment 1: SM	Experiment 2: PI	Experiment 3: SM + RS	Experiment 4: RS, PI
m	−0.0684 (0.0)	−0.0328 (0.0005)	−0.0360 (0.0003)	−0.0334 (0.003)
α	0.8542	0.9273	0.9204	0.9260

Randomisation can slow convergence in a single run, but, when averaged over many runs, convergence is very similar to fixed spring convergence.

The result that, when particle interactions and/or randomisation is included, the convergence factor α is close to the limiting value for convergence ($\alpha = 1.0$), may explain why a clamping velocity is often used in PSO implementations. For example, Eberhart and Shi (2000) recommend that each particle velocity is clamped, immediately after velocity update, to the dynamic range.

4.2 Diversity measure for charged particles

4.2.1 Experiment design

Experiments 5 and 6 investigate swarm spatial size for charged swarms (swarms with N neutral and M^+ charged particles of charge Q) for core radii $r_c = 1.0$ and 0.1 respectively. A (20, 20^+) swarm was used in both experiments, and 50 runs were completed in each case.

4.2.2 Results and analysis

Figures 7, 8, 9 and 10 show charged swarm size plotted against iteration. The mean, standard error, minimum and maximum values of $|S^+|$ are computed from iterations 100–1,000 to allow the charged swarm to stabilise. Figures 7 and 9 show $|S^+|$ for a single run. The figures demonstrate that the charged swarm, unlike the neutral swarm, is not contracting; however the charged swarm size is subject to large fluctuations, and the fluctuations are larger for smaller core radius. Figures 8 and 10 show the average $|S^+|$ over 50 runs. Fluctuations about the

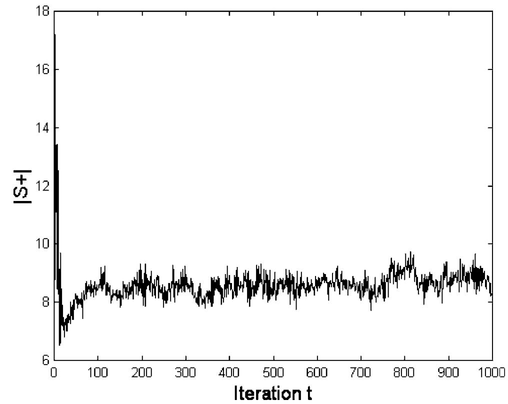

Fig. 8 Experiment 5, 50 runs, $r_c = 1.0$, mean size = 8.6080 (0.3353), min = 7.7166, max = 9.7166

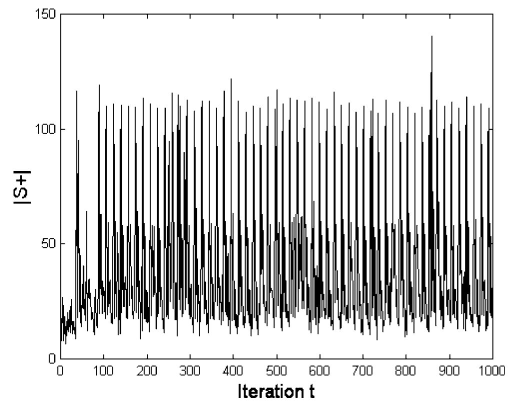

Fig. 9 Experiment 6, 1 run, $r_c = 0.1$, mean size = 41.6626 (29.0906), min = 8.4555, max = 140.4039

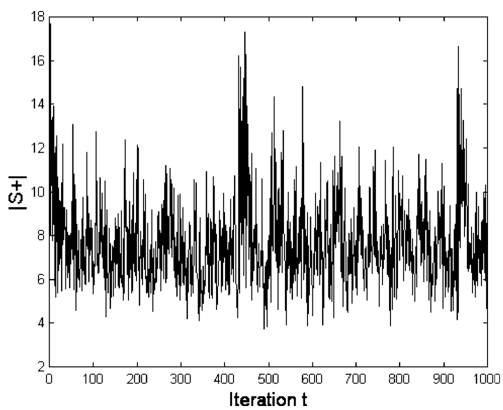

Fig. 7 Experiment 5, 1 run, $r_c = 1.0$, mean size = 7.6186 (2.0013), min = 3.7150, max = 17.2935

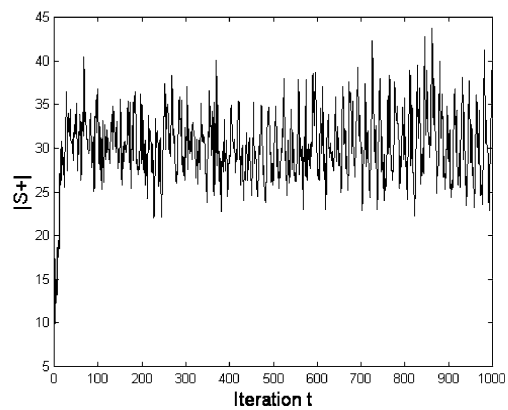

Fig. 10 Experiment 6, 50 runs, $r_c = 0.1$, mean size = 30.3736 (3.6213), min = 22.0341, max = 43.7421

Table 6 Charged swarm size for experiments 5 and 6

Experiment	r_c	r_p	$<\lvert S^+\rvert>$	$\lvert S^+\rvert_{min}$	$S^+\rvert_{max}$	$\lvert S^+\rvert_{lower}$	$S^+\rvert_{upper}$
5	1.0	10.0	8.61 (0.07)	3.25	24.34	0.91	28
6	0.1	10.0	30.4 (0.5)	4.6	602.7	1.9	1,900

$<\lvert S^+\rvert>$ is the mean size averaged over all 50 runs (standard error). The minimum and maximum swarm sizes achieved over the whole set of 50 runs is also shown. The first 100 iterations in each run are ignored. The final two columns show theoretical upper and lower bounds

mean $|S^+|$ are reduced when averaged, and this reduction is greater for $r_c = 1.0$.

Equations 22 and 23 provide estimates of the fluctuations in swarm size. Table 6 shows the results of computing these bounds for experiments 5 and 6. In order to obtain $|S^+|_{min}$, the estimated inter particle separation R is found by comparing $\chi\tilde{\phi}(= 2.992)$ with r_c and r_p, according to conditions 1–3 of Sect. 3.3.

The observed values for $|S^+|_{min/max}$are within the predicted bounds. The lower bound underestimates by factors of 2.4 and 3.6 due to R underestimating mean particle separations (velocity and many body effects are ignored). The upper bound for the $r_c = 1.0$ swarm is consistent with observations, but the same bound for the $r_c = 0.1$ swarm is 3.2 times too big. This is because the upper bound estimate is very sensitive to the core acceleration a_c which is large for the $r_c = 0.1$ swarm ($a_c = 100$).

The choice between these two swarms (or another swarm with a different r_c) depends on the extent of diversity required. In this case, the dynamic range is 10, and the $r_c = 1.0$ swarm covers some 80% of the search space in each dimension. However, the $r_c = 0.1$ swarm is very inefficient in this context since it extends far beyond the edge of the search space.

4.3 Optimum tracking

4.3.1 Experiment design

Two experiments, 7 and 8, test the ability of a (40, 0) neutral swarm and a (20, 20^+) swarm to track a moving optimum in environments of different severity. In each experiment, an offset vector (s, s, s) was added to the global minimum $\mathbf{x}_a$ of the sphere function $f_{sph}(\mathbf{x})$ at every 100th iteration. An offset of $s = 0.1$ was chosen for experiment 7. This is a mild change, representing a shift of just 1% of the dynamic range. Experiment 8 is more severe with $s = 5.0$, corresponding to a shift of 50% of the dynamic range. The experiments were repeated 50 times with different random number seeds. A subsidiary series of experiments, similar to experiment 2, was run in order to find the convergence factor, α, for the (40, 0) neutral swarm.

4.3.2 Results and analysis

The convergence factor for the neutral swarm was found to be 0.94. With an initial swarm size of 10, the expected swarm size at the 100th iteration is $10(0.94)^{100} = 0.021$. The optimum jump in experiment 7 is about five times the neutral swarm diversity and about 250 times for experiment 8.

The results for the dynamic experiments are shown in Figs. 11, 12, 13 and 14. The figures show the average over 50 runs of $|\mathbf{p}_g(t) - \mathbf{x}_a(t)|$, the Euclidean distance of the entire swarm's best position at iteration t, $\mathbf{p}_g(t)$, from the global minimum at $\mathbf{x}_a$.

Figures 11 and 12 show the results for the mild environment. The best position obtained by the neutral swarm improves between jumps, but overall the performance deteriorates. The charged swarm is better at tracking the optimum, and the performance is stable after the fifth jump. The results for the severe environment (Figs. 13, 14) show similar behaviour. The charged swarm performs relatively better in the severe environment because it has the same absolute error ($|\mathbf{p}_g - \mathbf{x}_a| = 0.1$) in the two environments. This is because optimum jump is always within the charged swarm—the swarm does not distinguish between the two environments.

5 Conclusions

If PSO is to be applied to a dynamic problem, then some knowledge of the rate of convergence of the swarm compared to the average jump in optimum position is desirable. If the swarm has a small diversity compared to the optimum change it will be difficult for the swarm to re-diversify and track the change. A simple diversity increasing mechanism, inter-particle repulsion between

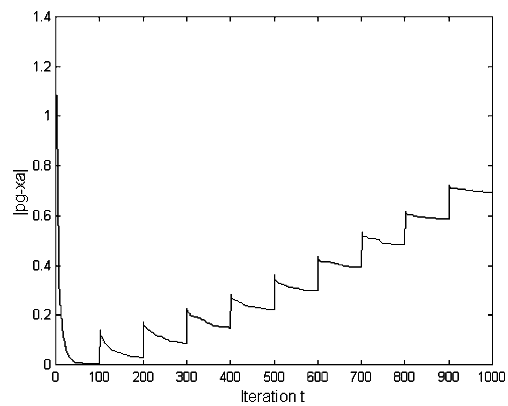

Fig. 11 Experiment 7—Neutral swarm, severity = 0.1

'charged' particles, has been suggested and shown to work well in some severe environments.

To help understand how a swarm of neutral particles—classic PSO—loses diversity, and how the inclusion of some charged particles to the swarm maintains diversity (CPSO), the maximum spatial extent of the swarm along any axis, swarm size $|S|$, is proposed as a suitable diversity measure.

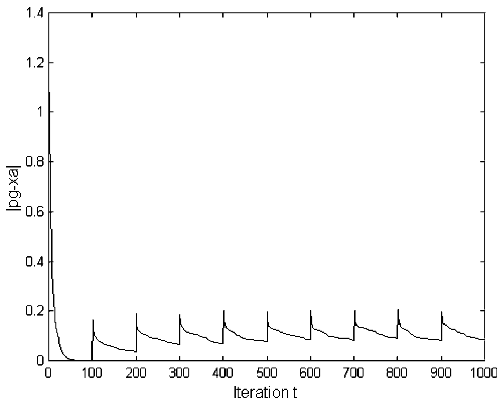

Fig. 12 Experiment 7—Charged swarm, severity = 0.1

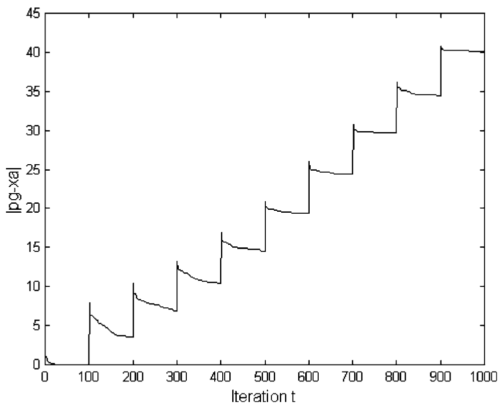

Fig. 13 Experiment 8—Neutral swarm, severity = 5

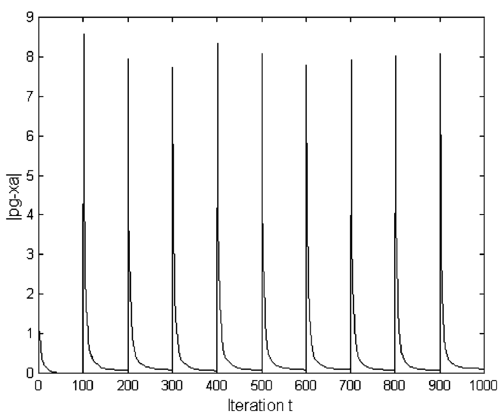

Fig. 14 Experiment 8–Charged swarm, severity = 5

Some analysis motivates, under conditions when convergence is towards a spherically symmetric optimum, a scaling law $|S| = k\alpha^{t}$. The convergence factor α is related to the constriction χ by $\alpha = (\eta\chi)^2$ where $\eta = 1$ for the simplified model, $\eta > 1$ otherwise.

The scaling law was demonstrated with a 20 particle swarm and the three-dimensional sphere function for four models: a simplified non-interacting model, the simplified model with interactions, the simplified model with spring randomisation and the full PSO.

The theoretical prediction $\eta = 1$ was verified for the simplified model. It was also discovered that the effects of particle interactions, random springs or both together (i.e. neutral PSO) were similar, each slowing convergence from $\alpha = 0.8542$ to $\alpha = 0.92$–0.93. The near critical convergence sheds light on the PSO folk-lore that velocity clamping is helpful even under constriction. Spring randomisation induces small fluctuations around scaling, slightly slowing convergence. It is already known that spring randomisation aids PSO convergence for harder objective functions, presumably due to diversity fluctuations.

It was predicted that the charged swarm would not collapse due to the balance between attraction towards the best positions found by the neutral particles, and repulsion amongst the charged particles. This was observed in experiments. Analysis of the charged swarm diversity suggested quite large fluctuations in swarm size $|S^{+}|$ and upper and lower bounds were proposed. These bounds depend on particle charge Q and two parameters of the modified Coulomb law, the core radius r_c and perception limit r_p.

Experiments with a 40 particle swarm, half of which are charged, reveal large fluctuations in $|S^{+}|$, although the average over 50 runs is smoother. At $r_c = 1.0$ the charged swarm covers the whole of the dynamic range X, but at $r_c = 0.1$ the charged particles spend much time outside this range. Although the smallest swarm sizes observed were similar for both parameters, the $r_c = 0.1$ swarm has very large fluctuations at some 60 times X. It would seem, therefore that the $r_c = 1.0$ charged swarm would be more efficient for problems where dynamism occurs within X. The calculated upper and lower limits give broad indications of these fluctuations.

Charged and neutral swarms were tested in a simple dynamic optimisation problem. As expected by the picture emerging from the theoretical and empirical study of diversity loss, the neutral swarm performed poorly in comparison with the charged swarm, both for mild and severe dynamism. The charged swarm tracked the jumping optimum to within the same absolute error in position for both environments, suggesting its potential versatility in environments of unknown diversity.

It should be noted that predictions for $|S|$ do not take into account asymmetric optima neighbourhoods. In such cases, an analysis using the maximum spatial extent along each axis, $|S_j|$, $j = 1,\ldots,d$, might be more appropriate. Although analysis did proposed upper and lower limits for $|S^{+}|$, and these were verified in the experiments, the best settings for Q, r_c, r_p and the relative number of charged particles is undetermined by theory and remains empirical.

References

Blackwell TM, Bentley PJ (2002) Dynamic search with charged swarms. In: Proceedings of genetic and evolutionary computation conference, pp 19–26

Blackwell TM (2003) Swarms in dynamic environments. In: Proceedings of genetic and evolutionary computation conference, pp 1–12

Branke J (2001) Evolutionary optimization in dynamic environments. Kluwer, Boston

Branke J (2003) Evolutionary approaches to dynamic optimization problems—introduction and recent trends. In: Branke J (ed) GECCO workshop on evolutionary algorithms for dynamic optimization problems, pp 2–4

Carlisle A, Dozier G (2000) Adapting particle swarm optimisation to dynamic environments. In: Proceedings of international conference on artificial intelligence, pp 429–434

Clerc M, Kennedy J (2002) The particle swarm: explosion, stability and convergence in a multi-dimensional complex space. IEEE Trans Evol Comput 6:158–73

Eberhart R, Shi Y (2000) Comparing inertia weights and constriction factors in particle swarm optimisation. In: Proceedings of congress on evolutionary computation, pp 84–88

Eberhart RC, Shi Y (2001) Particle swarm optimisation: developments, applications and resources. In: Proceedings of congress on evolutionary computation, pp 81–86

Eberhart RC, Shi Y (2001) Tracking and optimizing dynamic systems with particle swarms. In: Proceedings of congress on evolutionary computation, pp 94–97

Hu X, Eberhart RC (2002) Adaptive particle swarm optimisation: detection and response to dynamic systems. In: Proceedings of congress on evolutionary computation, pp 1666–1670

Kennedy J, Eberhart RC (1995) Particle swarm optimisation. Proc IEEE Int Conf Neural Netw 4:1942–1948